

$^2\Sigma^- \rightarrow X^2\Pi$, BAND SYSTEM IN PO MOLECULE

BY N. A. NARASIMHAM, M. N. DIXIT AND V. SETHURAMAN

(*Spectroscopy Division, Atomic Energy Establishment Trombay, 414 A, Cadell Road, Bombay-28*)

Received May 3, 1965

(Communicated by Dr. R. K. Asundi, F.A.Sc.)

INTRODUCTION

THE ultra-violet spectrum of PO was known to consist of two well-developed β - and γ -systems, the former extending from 3100–3600 Å and the latter from 2300–2800 Å. Singh (1959) and Suryanarayana Rao (1958) have analysed the rotational structure of these bands and shown that they arise from two $^2\Sigma$ states to a common $^2\Pi$ state which is the ground state of PO molecule. Recently, Santaram and Tiruvenganna Rao (1962) reported an extensive band system lying in the same region as the PO γ -system. About the same time, we had also obtained these bands and proposed an identical vibrational analysis independently but deferred the publication in order to complete the rotational analysis of the bands. We photographed these bands on a 6.6 metre concave grating spectrograph in the second and third orders which gave a much higher dispersion and resolution than the medium quartz instrument employed by Santaram and Tiruvenganna Rao. Studies including the rotational analysis of some of these bands are now completed and the results are presented in this paper.

EXPERIMENTAL

The PO bands are excited in a discharge through a few mm. of argon and traces of oxygen in a sealed quartz tube containing phosphorus. The quartz tube, about 10 cm. long and 15 mm. in diameter, is initially evacuated by a high vacuum system and degassed by heating for over an hour at 600–800° C. A small amount of phosphorus is then distilled into the tube and 1–2 mm. of argon and trace amounts of oxygen are introduced into it. The tube is then sealed off the vacuum system. A microwave oscillator of 2450 mc./s. is used to excite the discharge. The new bands are developed when the discharge is intense white.

The resulting spectra are photographed in the second order of a Jarrell-Ash 3.4 metre grating spectrograph at a dispersion of 2.5 Å/mm. and in 314

the second and third orders of 6.6 metre concave grating spectrograph at dispersions of 0.57 Å/mm. and 0.38 Å/mm. respectively. Kodak B-10 and O-a-O plates are used to photograph the bands. The new bands occur in the same region as the PO- γ bands but are comparatively weaker and degraded towards the red. A representative spectrogram of the bands taken on the Jarrell-Ash spectrograph is given in Fig. 1. The rotational structure for 0-2 band photographed on the 6.6 metre concave grating spectrograph in the third order is shown in Fig. 2.

RESULTS AND DISCUSSION

Most of the bands of the new system that lie in the region 2400–2800 Å are photographed on the 6.6 metre concave grating spectrograph. Vacuum wave numbers of the band heads measured on these plates are given in a Deslandres vibrational scheme in Table I. There still remain a few more bands and these are measured on plates taken on the Jarrell-Ash 3.4 metre grating spectrograph. These are also included in the Deslandres scheme and are shown with an asterisk.

(a) Vibrational Structure

The bands occur as doublets with an average separation 223.9 cm.⁻¹ which agrees well with the value known for the $^2\Pi$ ground state of PO. Further the $\Delta G_{v+\frac{1}{2}}$ and w_{ex} values for the lower state of the new bands agree closely with corresponding ground-state values of β - and γ -bands of PO. The R₁ and Q₂ heads could be expressed by the relation

$$\nu_h = \frac{43852.43}{628.60} \left\{ + 826.37(v' + \frac{1}{2}) - 6.96(v' + \frac{1}{2})^2 - [1233.38(v'' + \frac{1}{2}) - 6.56(v'' + \frac{1}{2})^2] \right\}$$

The positions of the band heads calculated from the above expression agree fairly well with the observed values as is evident from the not too significant differences between the observed and calculated values given in column 5 of Table II.

(b) Rotational Structure

Each sub-band shows two heads (Fig. 2). This coupled with the fact that the final level of the band system is a $^2\Pi$ state, indicates the initial level to be a $^2\Sigma$ or $^2\Delta$ state. For either transition, $^2\Sigma \rightarrow ^2\Pi$ or $^2\Delta \rightarrow ^2\Pi$ where $^2\Pi$ belongs to Hund's case (a), the following twelve branches are expected:

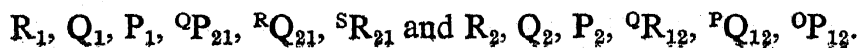


TABLE I
Deslandres scheme for the band heads of the new system of PO

V'	0	1	2	3	4	5	6	7	8	9	10	11	12	$\Delta G_V + \tau_{12}$
0	43658-20 ^a 49-10 ^b 1221-00	42438-44 28-10 1206-00	41232-35 21-22 1193-65	40039-60 27-57 1181-08	38859-41 46-51									
1	43435-20 ^a 812-00	42215-52 04-20 1228	41008-71 03-75 1181-11	39815-80 812-82	38635-13 812-62									
2	43251-80 ^a 812-40	40850-74 39-73 1180-68	39671-03 59-13 1187-71	386504-37 491-42 1154-34	37350-71 37-08									
3	43027-70 ^a 16-60 ^c		3880-70	37126-84										
4			67-30 1164-13	13-24										
5		42841-37 31-16 1193-70	41648-16 37-46	380148-07 34-82 1140-73	37007-76 36994-09 1124-67	36680-20 65-42								
6		42617-64 07-63 1193-66	41424-57 13-97	38677-61 65-64 1154-35	37924-07 11-29 1140-00	36783-18 70-31 1124-67	41-64							
7				41251-54 41-28	78-17 1128-77	49-40 1115-29	34-11 1101-51	32-50 ^d						
8		41027-60 17-29		41039-11 54-33 1124-68	36439-11 25-67 1115-32	35324-91 10-34 1101-54	34224-60 ^e	08-80 ^e						
9					37590-28	36663-16	35549-52	34449-80 ^f						
10					37566-54	36439-11	35324-91	34224-60 ^e						
11					41027-60 17-29	54-33 1124-68	35217-15	34130-00 ^f	33055-50 ^f					
12						04-53 1101-98	02-55 1048-65	13-90 1078-30	37-60 ^f					
13						36094-10 80-79 1101-69	34993-80 ^f 79-10 1048-60	33903-60 ^f 890-50 ^f						
14						756-10	756-50	757-10						
15									758-57					
16										34882-90 ^f	33810-80 ^f			
17										70-40 1075-70	794-70 ^f			
18										35748-70 ^f	3386-90 ^f			
19										36-20 ^f				
20														

$\Delta G_V + \tau_{12}$

$2\omega e X_0''$

$1221-00$

$1206-04$

$1193-56$

$1180-54$

$1167-71$

$1154-28$

$1140-85$

$1128-69$

$1115-31$

$1101-63$

$1098-67$

$1076-00$

$1072-31$

$1061-52$

$1042-63$

$1021-43$

$1001-64$

$981-55$

$961-46$

$941-37$

$921-28$

$901-20$

$881-11$

$861-02$

$841-03$

$821-14$

$801-25$

$781-36$

$761-47$

$741-58$

$721-69$

$701-80$

$681-91$

$661-92$

$641-93$

$621-94$

$601-95$

$581-96$

$561-97$

$541-98$

$521-99$

$501-100$

$481-101$

$461-102$

$441-103$

$421-104$

$401-105$

$381-106$

$361-107$

$341-108$

$321-109$

$301-110$

$281-111$

$261-112$

$241-113$

$221-114$

$201-115$

$181-116$

$161-117$

$141-118$

$121-119$

$101-120$

$81-121$

$61-122$

$41-123$

$21-124$

$01-125$

TABLE II

Vacuum wave numbers of R_1 and Q_2 heads of the bands of $^2\Sigma - X^2\Pi_{reg.}$ system of PO

The same have been calculated from the expression

$$\nu_h = \begin{cases} 43852.43 \\ 43628.60 \end{cases} + 826.37(v' + \frac{1}{2}) - 6.96(v' + \frac{1}{2})^2 - 1233.38(v'' + \frac{1}{2}) + 6.56(v'' + \frac{1}{2})^2$$

and their differences from the observed values are given in column 5.

$v' - v''$	Sub-heads	Wavelength in air Å	Wave-numbers in vacuum cm. ⁻¹	Observed—Calculated
0—0	R_1	2290.292	43649.10	+0.27
	Q_2	2302.102	43425.20	+0.20
1—1	R_1	2311.957	43240.10	-0.92
	Q_2	2323.970	43016.60	-0.59
2—2	R_1	2334.033	42831.16	-1.25
	Q_2	2346.277	42607.63	-0.95
0—1	R_1	2356.208	42428.10	-0.47
	Q_2	2368.709	42204.20	-0.54
2—3	R_1	2400.952	41637.46	-0.93
	Q_2	2413.910	41413.97	-0.59
3—4	R_1	2424.019	41241.28	-0.82
	Q_2	2437.257	41017.29	-0.98
0—2	R_1	2425.199	41221.22	-0.21
	Q_2	2438.440	40997.40	-0.20
1—3	R_1	2447.851	40839.79	-0.07
	Q_2
0—3	R_1	2497.525	40027.57	+0.16
	Q_2	2511.570	39803.75	+0.17
1—4	R_1	2520.729	39659.13	+0.17
	Q_2
2—5	R_1
	Q_2	2559.027	39065.64	-0.24
0—4	R_1	2573.463	38846.51	0.00
	Q_2	2588.380	38622.64	-0.04

Table II (*Contd.*)

$v' - v''$	Sub-heads	Wavelength in air Å	Wave-numbers in vacuum cm. ⁻¹	Observed—Calculated
1—5	R ₁	2597·205	38491·42	+0·24
	Q ₂	2612·410	38267·39	+0·04
2—6	R ₁	2621·493	38134·82	-0·23
	Q ₂	2636·951	37911·29	+0·07
3—7	R ₁	2646·243	37778·17	+0·05
	Q ₂	2662·017	37554·33	+0·04
1—6	R ₁	2677·507	37337·08	+0·56
	Q ₂	2693·657	37113·24	+0·55
2—7	R ₁	2702·333	36994·09	+0·58
	Q ₂	2718·780	36770·31	+0·63
3—8	R ₁	2727·750	36649·40	-0·30
	Q ₂	2744·505	36425·67	-0·20
4—9	R ₁	2753·663	36304·53	-0·56
	Q ₂	2770·740	36080·79	-0·47
5—10	R ₁
	Q ₂	2797·458	35736·20	+0·35
2—8	R ₁	2787·379	35865·42	+0·33
	Q ₂	2804·880	35641·64	+0·38
3—9	R ₁	2813·210	35534·11	-0·29
	Q ₂	2831·199	35310·34	-0·23
4—10	R ₁	2839·868	35202·55	-0·36
	Q ₂	2858·010	34979·10	+0·02
5—11	R ₁	2866·920	34870·40	-0·22
	Q ₂
3—1	0R ₁	2903·374	34432·60	+0·38
	Q ₂	2922·370	34208·80	+0·41
4—11	R ₁	2930·500	34113·90	+0·05
	Q ₂	2949·817	33890·50	+0·48
5—12	R ₁	2958·180	33794·70	+0·02
	Q ₂	2977·857	33571·40	+0·55
4—12	R ₁	3025·979	33037·60	-0·31
	Q ₂

For negligible spin splitting of the initial state, as has been noticed for the initial ${}^2\Sigma$ states of the β - and γ -systems of PO, the lines of branches Q_1 and ${}^0P_{21}$ blend together as do also those of R_1 and ${}^RQ_{21}$, Q_2 and ${}^0R_{12}$, P_2 and ${}^RP_{12}$. This reduces the total number of branches observed to only eight, as is indeed found to be the case in the bands analysed. These are shown in the Fortrat diagram in Fig. 3 for the 0-2 band. The positions of the rotational lines of a ${}^2\Sigma - {}^2\Pi$ (case *a*) transition are obtained from the following relations and plotted as circles against running J values (Fig. 3). The observed rotational structure of the corresponding sub-bands is shown below the diagram. All the expected rotational lines lie well within the calculated positions.

$$\begin{aligned}
 {}^S R_{21}(J) &= \nu_0^{(1)} + F_2'(J+1) - F_1''(J) \\
 &= \nu_0^{(1)} + \frac{15}{4}B' + (4B' - B^{(1)''})J^2 \\
 R_1(J) &= \nu_0^{(1)} + F_1'(J+1) - F_1''(J) \\
 &= \nu_0^{(1)} + \frac{3}{4}B' + (2B' - B^{(1)''})J + (B' - B^{(1)''})J^2 \\
 Q_1(J) &= \nu_0^{(1)} + F_1'(J) - F_1''(J) \\
 &= \nu_0^{(1)} - \frac{1}{4}B' - B^{(1)''}J + (B' - B^{(1)''})J^2 \\
 P_1(J) &= \nu_0^{(1)} + F_1'(J-1) - F_1''(J) \\
 &= \nu_0^{(1)} + \frac{3}{4}B' - (2B' + B^{(1)''})J + (B' - B^{(1)''})J^2 \\
 {}^0P_{21}(J) &= \nu_0^{(1)} + F_2'(J-1) - F_1''(J) \\
 &= \nu_0^{(1)} - \frac{1}{4}B' - B^{(1)''}J + (B' - B^{(1)''})J^2 \\
 {}^RQ_{21}(J) &= \nu_0^{(1)} + F_2'(J) - F_1''(J) \\
 &= \nu_0^{(1)} + \frac{3}{4}B' + (2B' - B^{(1)''})J + (B' - B^{(1)''})J^2 \\
 R_2(J) &= \nu_0^{(2)} + F_2'(J+1) - F_2''(J) \\
 &= \nu_0^{(2)} + \frac{15}{4}B' + (4B' - B^{(2)''})J + (B' - B^{(2)''})J^2 \\
 Q_2(J) &= \nu_0^{(2)} + F_2'(J) - F_2''(J) \\
 &= \nu_0^{(2)} + \frac{3}{4}B' + (2B' - B^{(2)''})J + (B' - B^{(2)''})J^2 \\
 P_2(J) &= \nu_0^{(2)} + F_2'(J-1) - F_2''(J) \\
 &= \nu_0^{(2)} - \frac{1}{4}B' - B^{(2)''}J + (B' - B^{(2)''})J^2 \\
 {}^0P_{12}(J) &= \nu_0^{(2)} + F_1'(J-1) - F_2''(J) \\
 &= \nu_0^{(2)} + \frac{3}{4}B' - (2B' + B^{(2)''})J + (B' - B^{(2)''})J^2
 \end{aligned}$$

$$\begin{aligned}
 {}^pQ_{12}(J) &= \nu_0^{(2)} + F_1'(J) - F_2''(J) \\
 &= \nu_0^{(2)} - \frac{1}{4}B' - B^{(2)''}J + (B' - B^{(2)''})J^2 \\
 {}^oR_{12}(J) &= \nu_0^{(2)} + F_2'(J+1) - F_2''(J) \\
 &= \nu_0^{(2)} + \frac{3}{4}B' + (2B' - B^{(2)''})J + (B' - B^{(2)''})J^2.
 \end{aligned}$$

TABLE III

Wave-numbers, in cm.^{-1} of the lines of the 0-2 band of the new ${}^2\Sigma^- - X^2\Pi_{\text{reg.}}$ system of PO

J	${}^sR_{21}$	${}^2\Sigma^- - X^2\Pi_{1/2}$ sub-band			${}^2\Sigma^- - X^2\Pi_{3/2}$ sub-band		
		R ₁	Q ₁	P ₁	R ₂	Q ₂	P ₂
4½	41228.71
5½	29.80
6½	30.57	41220.44	41211.50*
7½	31.32	19.93	09.69*
8½	31.92	19.13	07.76*
9½	32.23	18.27	05.49*	94.69	40981.87
10½	..	17.16	03.28	93.57*	79.43
11½	..	16.03	00.80	92.30	76.98
12½	32.46	14.73	198.15	41182.71	41008.87	90.92*	74.23
13½	32.23	13.17	95.42	78.60	..	89.29	71.37
14½	31.92	11.50*	92.43	74.42	..	87.55	68.31
15½	31.32	09.69*	89.33	70.08	07.22	85.56	65.05
16½	30.57	07.76*	86.13	65.68	06.31	83.38	61.71
17½	29.80	05.49*	82.71	60.95	05.30	81.04	58.15
18½	28.71	..	79.14	56.11	04.19	78.63	54.47
19½	27.58	..	75.48	51.13	02.77	76.03	50.51
20½	26.35	..	71.58	46.07	01.13	73.21	46.51
21½	24.89	..	67.58	40.78	40999.42	70.24	42.25
22½	23.09	..	63.36	..	97.43	67.17	37.84
23½	58.94	29.52	95.70*	63.80	33.34
24½	54.42	23.97	93.57*	60.47	28.59
25½	49.76	17.95	90.92*	56.77	23.61
26½	44.97	11.88	..	52.72	18.56
27½	40.00	48.81	13.34
28½	34.81	44.66	07.98
29½	29.52	40.33	02.33
30½	23.97	35.86	40896.57
31½	18.33	31.40	90.65
32½	12.68	26.28	84.55

* Blended lines.

TABLE III (Contd.)

Wave-numbers in cm^{-1} of the lines of the $^2\Sigma^- - X^2\Pi_{\frac{1}{2}}$ component
of the 0-3 band of the new $^2\Sigma^- - X^2\Pi_{\text{reg.}}$ system of PO

J	^s R ₂₁	R ₁	Q ₁	P ₁
4½
5½
6½
7½
8½	40013.51	..
9½	40038.82	40024.83	11.87	..
10½	39.29	23.84	09.81	..
11½	39.56	22.79	07.50	..
12½	..	21.64	05.00	..
13½	39.56	20.25	02.41	..
14½	39.29	18.87	39999.64	..
15½	38.82	17.23	96.81	..
16½	38.36	15.49	93.80	..
17½	37.75	13.51	90.65	..
18½	36.92	11.39	87.13	..
19½	35.97	09.12	83.63	..
20½	34.76	06.69	79.92	..
21½	33.50	04.20	76.16	..
22½	..	91.66	72.35	..
23½	..	98.76	68.16	..
24½	..	95.76	64.02	..
25½	..	92.63	59.50	..
26½	..	89.28	54.85	..
27½	..	86.02	50.31	..
28½	45.51	..
29½	40.53	..
30½	35.48	..
31½	30.23	..

(c) *A*-Type Doubling in the Ground State $X^2\Pi$

Vibrational analysis of the bands showed that the final level of the new system is the ground $^2\Pi_{\text{reg.}}$ state with a separation of 223.9 cm^{-1} . The $^2\Pi_{\frac{1}{2}}$ substate which forms the $F_1(J)$ series shows an appreciable *A*-doubling. As a result of this, the combination relations $R_1(J) - Q_1(J + 1)$ and $Q_1(J) - P_1(J + 1)$ are no longer found to be equal. In fact,

$R_1(J) - Q_1(J + 1)$ values are smaller than the $Q_1(J) - P_1(J + 1)$ values, as can be seen from the combination differences given in columns 2 and 4 of Table IV. Corresponding differences for the sub-bands involving $^2\Pi_{3/2}$ state, however, agree within the accuracy of the measurements (columns 6 and 7 of Table IV) indicating negligible A -doubling, as expected for the $^2\Pi_{3/2}$ state.

The β - and γ -systems are known to have for their final level the same $X^2\Pi$ ground state of the PO molecule. Rotational analysis of the sub-bands $^2\Sigma - ^2\Pi_{\frac{1}{2}}$ shows a combination defect which is due to the A -type doubling of the $^2\Pi_{\frac{1}{2}}$ state. A comparison of the combination defects, *viz.*, $[R_1(J) - Q_1(J + 1)] - [Q_1(J) - P_1(J + 1)]$ of the 1-2 and 2-3 bands of the γ -system with corresponding differences of the 0-2 and 0-3 bands of the present system (Table V) shows that they are about the same in magnitude but differ in sign. They are positive in the γ -system (as also in the β -system) and negative in the new system. Such a situation is possible if the parities of the initial $^2\Sigma$ states are different. This is evident from a study of the energy level diagram (Fig. 4) where transitions from $^2\Sigma^+$ and $^2\Sigma^-$ are shown to the common final level $^2\Pi$. A similar situation is obtained in the NO spectrum for the $A^2\Sigma^+ - X^2\Pi$ and $G^2\Sigma^- - X^2\Pi$ transitions (Lofthus and Miescher, 1964). If $^2\Sigma^+$ is assumed to be the initial state of the γ -system, which is most likely from considerations of the electronic configuration (3) given in the following section (e), the initial state of the new system becomes $^2\Sigma^-$. The new band system, then, arises out of a $^2\Sigma^- - X^2\Pi$ transition.

(d) Evaluation of the Rotational Constants

(i) *Initial $^2\Sigma^-$ state.*—The 0-2 and 0-3 bands which are relatively free from overlap have been analysed. Both the bands arise out of the zero vibrational level of the initial $^2\Sigma^-$ state and so only one set of B_0 and D_0 can be evaluated from $\Delta_1 F'_{av}(N)$ and $\Delta_2 F'_{av}(N)$ values. The combination differences used for these $\Delta F'$ values are shown below:

$$\Delta_1 F'_1(N + \frac{1}{2}) = R_1(N) - Q_1(N) = Q_1(N + 1) - P_1(N + 1)$$

$$\Delta_1 F'_2(N + \frac{1}{2}) = R_2(N) - Q_2(N) = Q_2(N + 1) - P_2(N + 1).$$

The average of the two first differences gives

$$\Delta_1 F'(N + \frac{1}{2}) = 2B_0'(N + 1) - 4D_0'(N + 1)^3.$$

The second differences give

$$\Delta_2 F'(N) = 4 B_0'(N + \frac{1}{2}) - 8 D_0'(N + \frac{1}{2})^3.$$

From these relations, B_0 is determined graphically and given in Table VI.

TABLE IV

*Combination differences for lower state of the 0-2 band at 2424.5 Å
of the new $^2\Sigma - X^2\Pi$ system of PO*

For comparison corresponding combination differences obtained from the 1-2 band of PO γ -system are also given.

J	$\Delta_1 F_1''(J+\frac{1}{2})$	$\Delta_2 F_1''(J)$	$\Delta_1 F_2''(J+\frac{1}{2})$	$\Delta_2 F_2''(J)$
	$R_1(J) - Q_1(J+1)$	$Q_1(J) - P_1(J+1)$	$R_2(J) - P_2(J+1)$	$R_2(J-1) - P_1(J+1)$
Present	PO- γ	Present	PO- γ	Present
5½
6½	10.75
7½	12.17
8½	13.64	13.65
9½	14.99	15.06	14.98	13.73
10½	16.36	16.54	16.31	15.15
11½	17.88	18.02	18.09	16.59
12½	19.31	19.39	19.55	18.07
13½	20.74	20.84	21.00	19.55
14½	22.17	22.32	22.35	20.98
15½	23.56	23.71	23.65	20.91
16½	25.05	25.21	25.28	20.91
17½	26.35	26.59	26.60	20.91
18½	..	28.04	28.01	20.91
19½	..	29.42	29.41	20.91
20½	..	30.80	30.80	20.91
21½	..	32.27	32.27	20.91
22½	..	33.68	33.73	20.91
23½	..	35.08	34.97	20.91
24½	..	36.44	36.47	20.91
25½	..	37.97	37.83	20.91
26½	20.91
27½	20.91
28½	20.91
29½	20.91
30½	20.91

TABLE IV (*Contd.*)

For comparison corresponding combination differences obtained from 2-3 band of PO- γ system are also given.

J	$\Delta_1 F_1''(J)$			
	$R_1(J) - Q_1(J + 1)$ from	$PO-\gamma$	$Q_1(J - P_1(J + 1))$ from	
	Present system	Present system	PO- γ	
8½
9½	15.02	15.05	..	14.88
10½	16.34	16.48	..	16.34
11½	17.79	17.91	..	17.70
12½	19.23	19.33	..	19.16
13½	20.61	20.76	..	20.56
14½	22.06	22.20	..	21.98
15½	23.43	23.56	..	23.24
16½	24.84	25.04
17½	26.38	26.47
18½	27.76	28.13
19½	29.20	29.41
20½	30.53	30.77
21½	31.85	32.15
22½	33.50	33.62
23½	34.74	35.01
24½	36.26	36.44
25½	37.78	37.85
26½	38.97	39.28
27½	40.51	40.74

(ii) *Final X²Π state.*—The B_v'' values for $v'' = 2$ and 3 are obtainable from a rotational analysis of the 0-2 and 0-3 bands of the present band system. The following combination relations of the rotational lines give the $\Delta_1 F$ and $\Delta_2 F$ values from which B_v and D_v are determined graphically in the usual manner (see for example, Herzberg, 1950) and given in Table VI.

$$\begin{aligned}\Delta_1 F_1(J + \frac{1}{2}) &= R_1(J) - Q_1(J + 1) = Q_1(J) - P_1(J + 1) \\ &= 2B_v^{(1)}(J + 1) - 4D_v^{(1)}(J + 1)^3\end{aligned}$$

$$\begin{aligned}\Delta_1 F_2(J + \frac{1}{2}) &= R_2(J) - Q_2(J + 1) = Q_2(J) - P_2(J + 1) \\ &= 2B_v^{(2)}(J + 1) - 4D_v^{(2)}(J + 1)^3\end{aligned}$$

TABLE V. Combination differences of the upper state $^2\Sigma^-$ obtained from the 0-2 and 0-3 bands of the new system of PO

$^2\Sigma^- \rightarrow X^2\Pi$, Band System in PO Molecule

325

N	$\Delta_1 F_1' (N)$			$\Delta_1 F_2' (N)$			$\Delta_2 F_1' (N)$			$\Delta_2 F_2' (N)$		
	$R_1(N) - Q_1(N)$	$Q_1(N+1) - P_1(N+1)$	$R_{21}(N-1) - R_1(N-1)$	$R_2(N) - Q_2(N)$	$Q_2(N+1) - P_2(N+1)$	$R_1(N) - P_1(N)$	$R_{21}(N-1) - Q_1(N-1)$	$R_2(N) - P_2(N)$	$R_2(N) - P_2(N)$	$R_2(N) - P_2(N)$	$R_2(N) - P_2(N)$	$R_2(N) - P_2(N)$
	0-2	0-3	0-2	0-2	0-3		0-2	0-2	0-2	0-3	0-2	0-2
5
6	8.94
7	10.24	10.13	19.07
8	11.37	11.39	21.63
9	12.78	12.96	..	12.79	12.82	..	24.16
10	13.88	14.03	..	13.96	13.99	..	14.14	..	26.74	26.95
11	15.23	15.29	15.44	..	15.45	..	15.52	29.48
12	16.58	16.64	16.82	..	16.77	..	16.69	32.02	..	32.06
13	17.75	17.84	18.01	17.73	..	17.95	17.92	34.57	34.64	..
14	19.07	19.23	19.25	19.06	19.31	..	19.24	37.12	36.81	37.15
15	20.36	20.42	20.42	20.42	20.42	..	20.51	39.61	39.49	39.63
16	21.63	21.69	21.76	21.63	21.59	21.66	21.67	42.08	41.99	42.01	42.17	..
17	22.78	22.86	23.03	22.81	22.87	22.93	22.89	..	44.44	44.56	44.60	..
18	..	24.26	24.35	24.31	24.24	24.26	24.16	..	47.09	47.10	47.15	..
19	..	25.49	25.51	..	25.53	25.56	25.52	..	49.57	49.79	49.72	..
20	..	26.77	26.80	..	26.85	26.74	26.70	..	52.10	52.34	52.26	..
21	..	28.04	28.07	27.92	27.99	..	54.77	54.84	54.62	..
22	..	29.31	29.42	..	29.30	29.18	29.33	..	57.31	57.34	57.17	..
23	..	30.61	30.45	30.26	30.46	..	69.73	..	69.59	..
24	..	31.74	31.81	31.90	31.88	62.36	..
25	..	33.13	33.09	33.10	33.16	64.98	..
26	..	34.43	34.15	34.16	67.31	..
27	..	35.71	35.47
28	36.68
29	38.00
30	39.29
31	40.75
32	41.73

$$\begin{aligned}\Delta_2 F_1(J) &= R_1(J-1) - P_1(J+1) \\ &= 4B_v^{(1)}(J + \frac{1}{2}) - 8D_v^{(1)}(J + \frac{1}{2})^3 \\ \Delta_2 F_2(J) &= R_2(J-1) - P_2(J+1) \\ &= 4B_v^{(2)}(J + \frac{1}{2}) - 8D_v^{(2)}(J + \frac{1}{2})^3\end{aligned}$$

where F_1 , $B^{(1)}$ and $D^{(1)}$ refer to the $^2P_{1/2}$ state and F_2 , $B^{(2)}$ and $D^{(2)}$ to $^2P_{3/2}$ state.

(iii) *Spin doubling constant, A.*—The spin doubling of the $X^2\Pi$ state has been determined from the relation

$$F_2''(J) - F_1''(J) = {}^S R_{21}(J) - R_2(J) = B_p'' [4(J + \frac{1}{2})^2 + Y(Y - 4)]^{\frac{1}{2}}$$

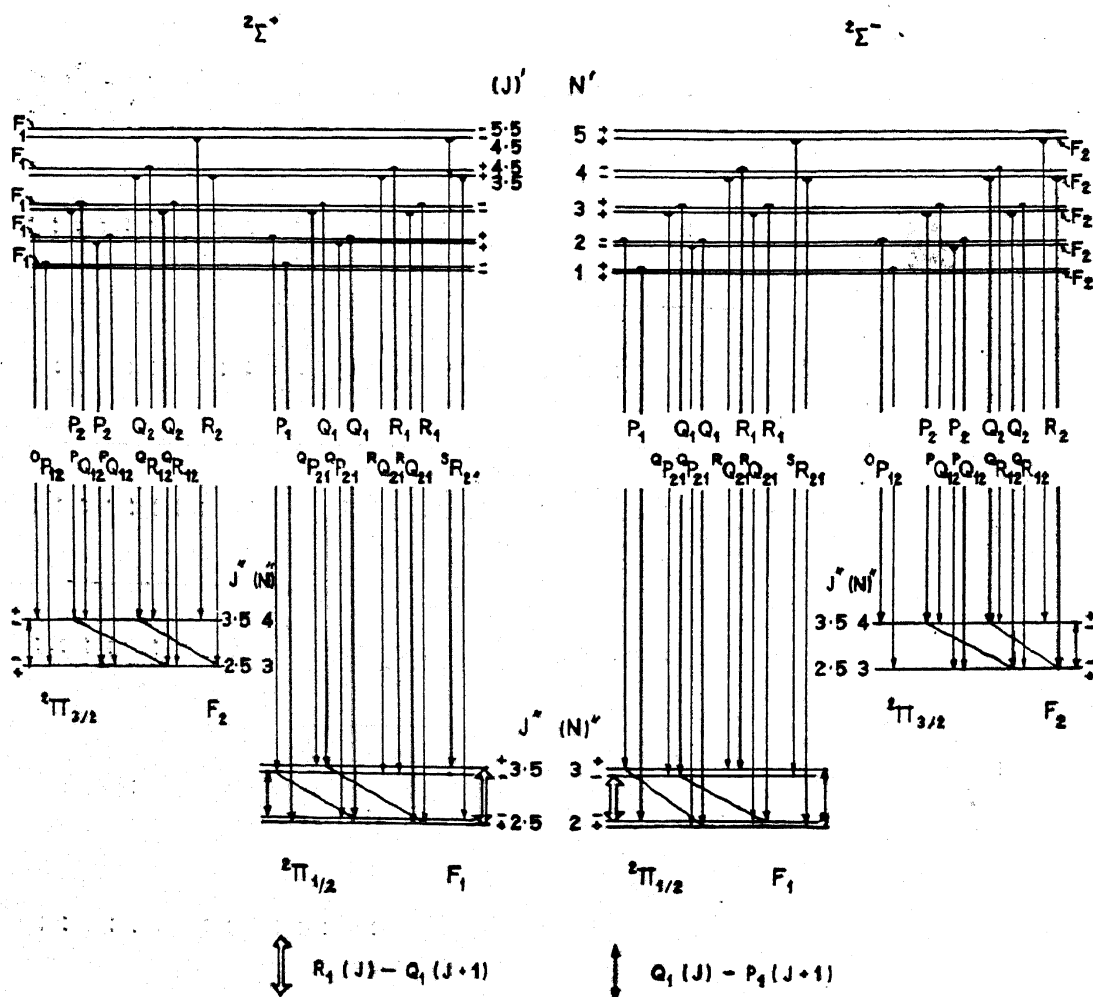


FIG. 4. Energy level diagram of transitions from $^2\Sigma^+$ and $^2\Sigma^-$ to a common $^2\Pi$ (case *a*) state.

where $Y = A/B_v$ and A is the coupling constant.

A plot of $[\{F_2''(J) - F_1''(J)\}/B_v'']^2$ against $(J + \frac{1}{2})^2$ gives an intercept of $Y(Y - 4)$ on the ordinate axis. The value of A evaluated from Y is also given in Table VI.

(e) *Electron configuration*

The PO molecule is isoelectronic with NS and its electron configuration for the ground state may be written down as

$$KKL(z\sigma)^2(y\sigma)^2(x\sigma)^2(w\pi)^4 v\pi \cdots X^2\Pi_{\text{reg.}} \quad (1)$$

TABLE VI

(i) *Vibrational and rotational constants of the upper $^2\Sigma^-$ state in cm^{-1}*

	Present work	Santaram and P. T. Rao
w_e'	826.37	825.8
$w_e' x_e'$	6.96	6.44
B_0'	0.637 ₈	..
r_0'	1.582, Å	..

(ii) *Vibrational and rotational constants of the Lower $^2\Pi$ state in cm^{-1}*

	Present work	K. Suryanarayana Rao	Santaram and P. T. Rao
w_e''	1233.38	1233.42	1232.6
$w_e'' x_e''$	6.56	6.57	6.48
Doublet separation	223.83	223.8	223.1
$B_2^{(1)''}$	0.718 ₇	0.719 ₂	..
$B_2^{(2)''}$	0.721 ₂		..
$B_3^{(1)''}$	0.713 ₅	0.714 ₀	..
α	0.005 ₂	0.005 ₆	..
A_2	224.22	224.33	..

Of the known excited states of PO, the β -, γ -and the new systems have their initial states lying at 30846, 40408 and 43853 cm. $^{-1}$ respectively above the ground state, $X^2\Pi_{reg.}$. The internuclear distances in the initial states, $^2\Sigma^+$ of the β -system and $^2\Sigma^-$ of the new system, increase on excitation from r_e of ground state. This may be understood to result from an excitation of one of the electrons from the $x\sigma$ bonding orbital to the antibonding $v\pi$ orbital. This gives rise besides others, to one $^2\Sigma^+$ and one $^2\Sigma^-$ states.



The promotion of the $v\pi$ antibonding electron from the ground electronic configuration (1) to a bonding $u\sigma$ orbital gives rise to a $^2\Sigma^+$ state



and this may be identified with the initial state of the γ -system. This is in accord with the expected decrease in the internuclear distance in the initial state of the γ -system.

Attempts were made in the early stages of this investigation, to spot bands due to the transition from the initial state of the new system at 43853 cm. $^{-1}$ to the $^2\Sigma^+$ of the β -system at 30846 cm. $^{-1}$. But these were not successful. This is now understandable since such a transition would, due to violation of $\Sigma^- \leftrightarrow \Sigma^+$ rule, be a forbidden one.

SUMMARY

The new ultra-violet bands of PO lying in the region 2300–3000 Å and degraded to the red, have been excited in a microwave (2450 mc./s.) discharge and photographed in the second and third orders of 3.4 m. and 6.6 m. grating spectrographs. Vibrational analysis of the R_1 and Q_2 heads shows that they can be expressed by the relation

$$\nu_h = \left. \begin{array}{l} 43852.43 \\ 628.60 \end{array} \right\} + 826.37(v' + \frac{1}{2}) - 6.96(v' + \frac{1}{2})^2 - \{1233.38(v'' + \frac{1}{2}) - 6.56(v'' + \frac{1}{2})^2\}.$$

Rotational analysis of the 0–2 and 0–3 bands shows that they arise out of a $^2\Sigma^- - X^2\Pi$ transition.

The vibrational and rotational constants are

(a) $^2\Sigma^-$ (initial) state

$$w_e' = 826.37 \text{ cm.}^{-1}$$

$$B_0' = 0.637 \text{ cm.}^{-1}$$

$$w_e'x_e' = 6.96 \text{ cm.}^{-1}$$

$$r_0' = 1.582 \text{ \AA}$$

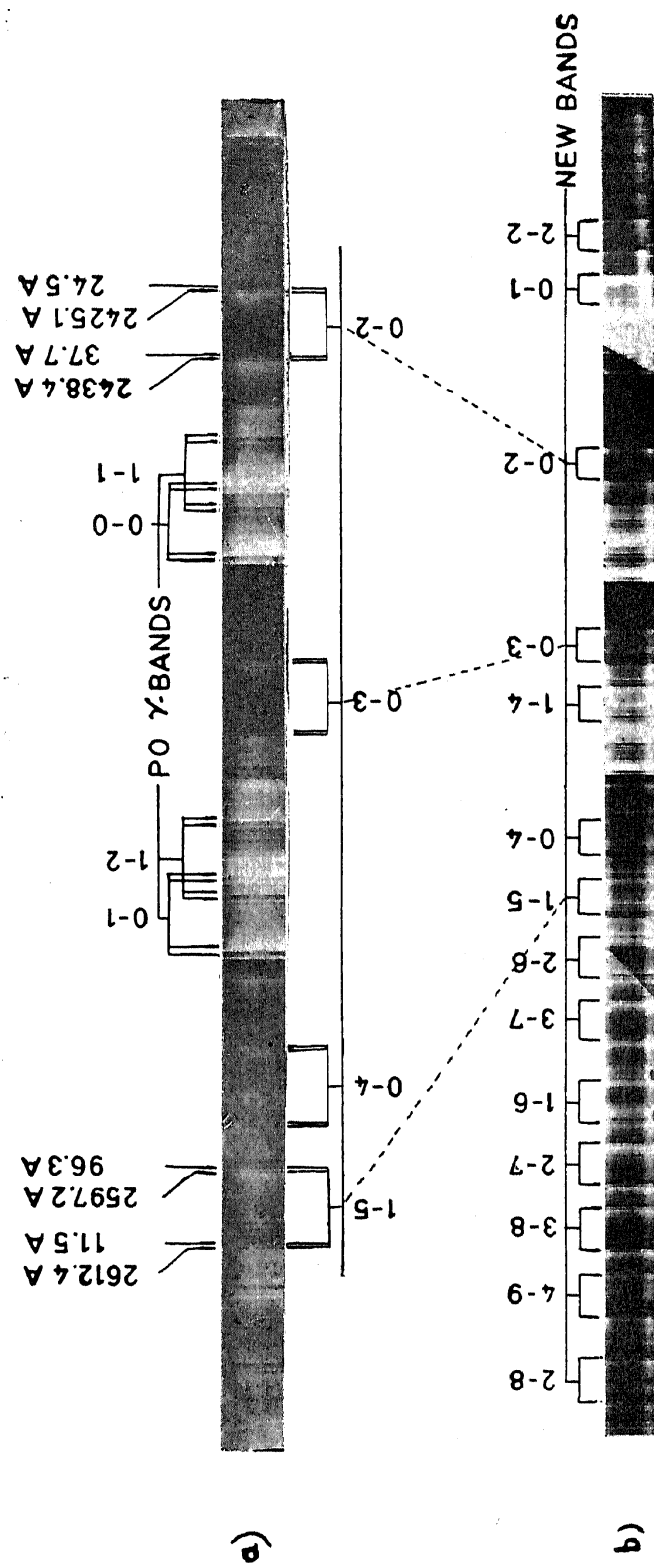


FIG. 1

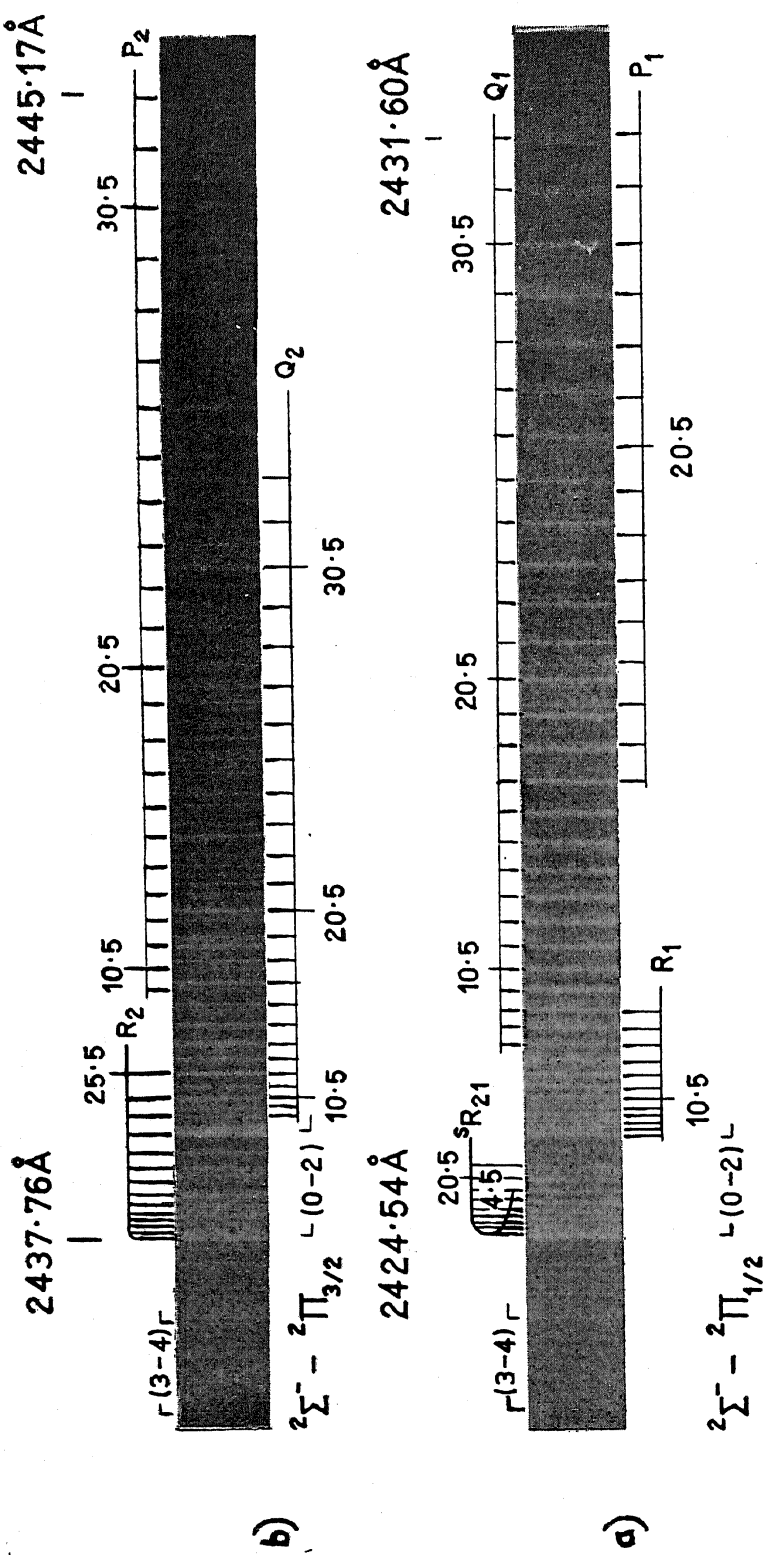
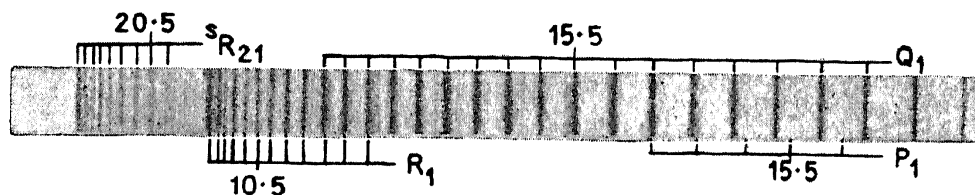
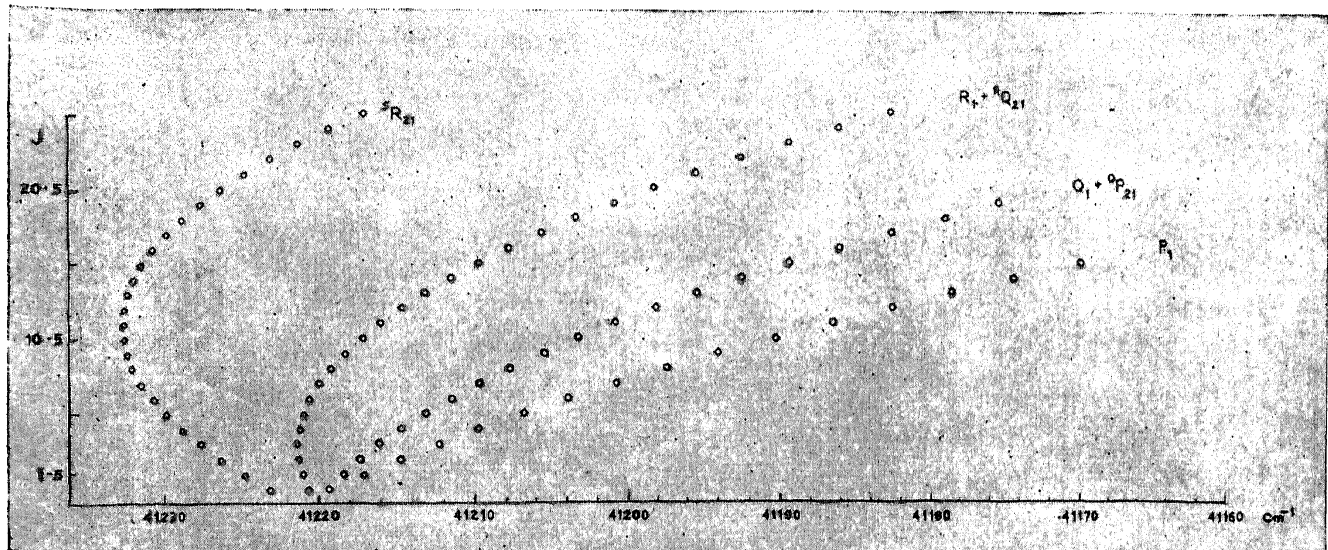


FIG. 2

$$^2\Sigma - ^2\Pi_{1/2}$$



$$^2\Sigma - ^2\Pi_{3/2}$$

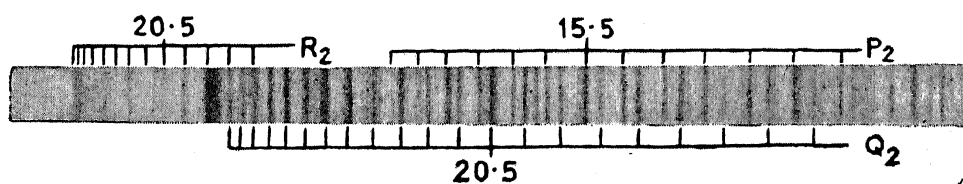
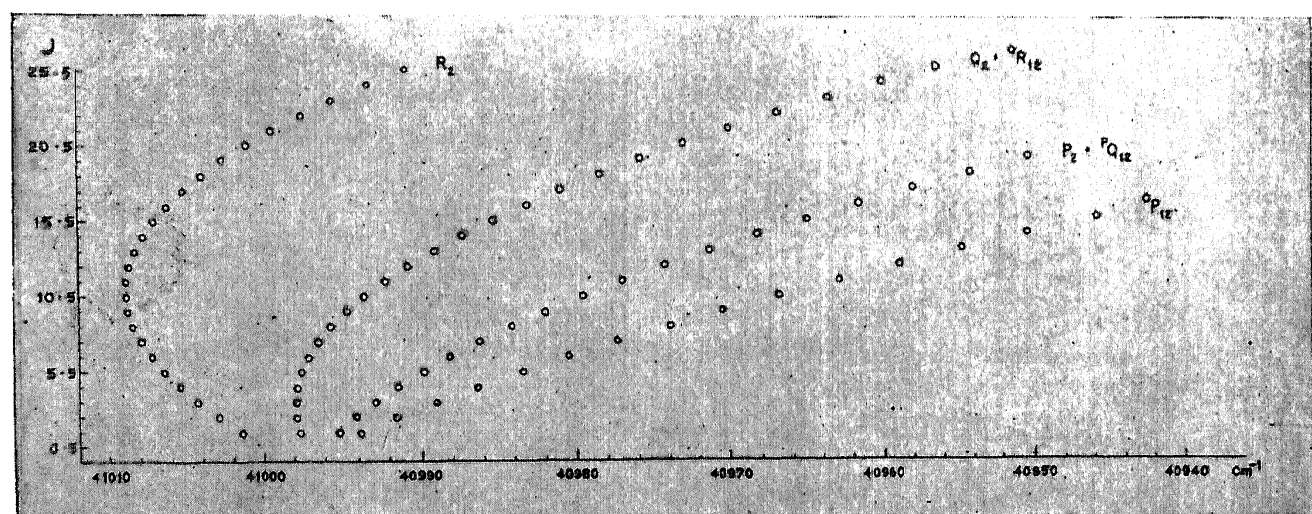


FIG. 3

(b) $X^2\Pi$ (final) state

$$w_e'' = 1233 \cdot 38 \text{ cm.}^{-1} \quad w_e''x_e'' = 6 \cdot 56 \text{ cm.}^{-1}$$

$$B_2'' = 0 \cdot 719_s \quad \alpha = 0 \cdot 005_2 \text{ cm.}^{-1}$$

Coupling constant $A_2 = 224 \cdot 22 \text{ cm.}^{-1}$

ACKNOWLEDGEMENT

We are indebted to Professor R. K. Asundi for a critical discussion of the manuscript and many helpful suggestions.

REFERENCES

- Singh, N. L. .. *Can. J. Phys.*, 1959, **37**, 136.
 Suryanarayana Rao, K. .. *Ibid.*, 1958, **36**, 1526.
 Santaram, C. V. V. S. N. K. and Tiruvenganna Rao, P. *Zeit. f. Phys.*, 1962, **168**, 553.
 Lofthus, A. and Miescher, E. *Can. J. Phys.*, 1964, **42**, 848.
 Herzberg, G. .. *Molecular Spectra and Molecular Structure*, D. Van Nostrand. Second Edition, 1950, 1.

EXPLANATION OF PLATES

PLATE V

FIG. 1. The new bands of PO photographed on the Jarrell-Ash 3.4 m. grating spectrograph. (a) is an enlargement of some of the bands in (b). The strong system of PO-γ overlaps bands of the new system.

PLATE VI

FIG. 2. Rotational structure of the 0-2 band of the $^2\Sigma^- - X^2\Pi$ system

- (a) $^2\Sigma^- - X^2\Pi_{1/2}$ sub-band,
 (b) $^2\Sigma^- - X^2\Pi_{3/2}$ sub-band.

The 3-4 band which is weak, lies on the shorter wavelength side of the 0-2 band.

PLATE VII

FIG. 3. Fortrat diagram of the 0-2 band of the $^2\Sigma^- - X^2\Pi$ system. The positions of the rotational lines are plotted against running J values. The observed rotational structure of the two sub-bands shown below the Fortrat diagram is found to be in good agreement with their calculated positions.